

**New Fe(III) trichlorido complex of a bidentate N'-(thiophen-2-ylmethylene)isonicotinohydrazide ligand: Synthesis, X-ray structure, spectral characterization, and electrochemistry study**

---

**ABSTRACT**

Fe(III) complex of the hydrazone from (*E*)-*N*'-(thiophen-2-ylmethylene)isonicotinohydrazide (HL) has been synthesized and characterized by elemental analysis, electrical conductance in non-aqueous solvents, FT-IR and electronic spectroscopies, room temperature magnetic measurement, electrochemistry study as well as by X-ray diffraction structure determination. In the complex, the ligand acts in its neutral bidentate form, coordinating through the carbonyl oxygen and azomethine nitrogen. A high spin octahedral geometry assigned to the Fe(III) complex were further confirmed by room temperature magnetic moment data. Elemental analysis showed that Fe(III) complex is composed of metal and ligand-ligands in a molar ratio of 1:1. This complex of Fe(III) is a neutral electrolyte in DMF solution. The electrochemistry study shows that a one-electron process determined the electrochemical reaction is governed by an electron transfer with an irreversible process. The structure of the complex has also been determined by X-ray diffraction revealing an octahedral environment around the Fe(III) ion.

*Keywords: Schiff base, iron(III), crystal, FTIR, electrochemistry*

**1. Introduction**

Schiff bases hydrazones form a class of organic compounds which are synthesized by the reaction condensation of a compound of type  $R_1R_2C=NNH_2$  and compound-compounds of type  $R_3R_4C=O$  or  $R_5HC=O$ . These compounds which can present donor sites such as O, N, or S are useful ligands largely used in coordination chemistry. Depending on their topology and the nature of the substituents, they can act with the metal ion in a bidentate, tridentate or tetradentate fashions. These types of ligands can act in neutral or deprotonated forms because the keto-enol tautomerization which can occur in solution as well as in solid state [1–4]. Schiff bases derived from nicotinic or isonicotinohydrazide are widely studied in coordination chemistry for their ability to bind metals ions through the azomethine nitrogen atom, the carbonyl oxygen atom as well as the pyridine nitrogen atom [5–11]. These facts increase the interest of the coordination chemists in these ligands and their analogues. Research papers involving transition metals and nicotinic or isonicotinohydrazide reported compounds with interesting properties such as fluorescence [12–14], magnetism [15], scavenger activity on superoxide radical [16], antibacterial [17, 18], catalytic [19, 20] and antitumoral [21, 22]. In this

regard, as part of our study on the hydrazones complexes [23–29] we prepared and characterized the hydrazone ligand (*E*)-*N'*-(thiophen-2-ylmethylene)isonicotinohydrazide (HL) and its Fe(III) complex and we studied the structure of the compounds and their electrochemistry properties.

## 2. Experimental Methods

2-thiophenecarbaldehyde, isonicotinic acid hydrazide, and  $\text{FeCl}_2 \cdot 4\text{H}_2\text{O}$  were purchased from Aldrich and used without further purification. Solvents were of reagent grade and were purified by the usual methods. Elemental analyses were performed in a Carlo-Erba EA microanalyzer. Infrared spectra were recorded with a FTIR Spectrum Two of Perkin Elmer spectrometer in the  $4000\text{--}400\text{ cm}^{-1}$  region. The  $^1\text{H}$  and  $^{13}\text{C}$  NMR spectra were recorded in  $\text{dms}\text{-}d_6$  on a Bruker 500 MHz spectrometer at room temperature using TMS as an internal reference. The UV–Vis spectra were run on a Perkin-Elmer UV/Visible spectrophotometer Lambda 365 spectrophotometer (1000–200 nm). The molar conductance of  $10^{-3}\text{ M}$  in DMF solution of the metal complex was measured at  $25\text{ }^\circ\text{C}$  using a WTW LF-330 conductivity meter with a WTW conductivity cell. The room temperature magnetic susceptibility of the complex was measured using a Johnson Matthey scientific magnetic susceptibility balance {calibrant  $\text{Hg}[\text{Co}(\text{SCN})_4]$ }. Melting points were recorded on a Büchi apparatus and are incorrect.

### 2.1. Synthesis of the ligand (*E*)-*N'*-(thiophen-2-ylmethylene)isonicotinohydrazide (HL)

Dissolve 2 g (14.58 mmol) of isonicotinic hydrazide in a flask containing 30 mL of methanol, add 2.4 g (21.14 mmol) of 2-thiophene-carboxaldehyde and two drops of glacial acetic acid. The reaction mixture is refluxed for 3 hours. The clear solution thus obtained is filtered while hot. After cooling, the white precipitate which appears is washed with methanol and then dried in a desiccator containing  $\text{P}_2\text{O}_5$ . Yield: 80%. Tf:  $> 260\text{ }^\circ\text{C}$ . Anal. calcd. for  $\text{C}_{11}\text{H}_9\text{N}_3\text{OS}$ : % C 57.13; % H 3.92; % N 18.17; % S 13.86. Found: % C 57.11; % H 3.90; % N 18.15; % S 13.86. IR ( $\nu$ ,  $\text{cm}^{-1}$ ): 1662 [ $\nu(\text{C}=\text{O})$  amide]; 1630 [ $\nu(\text{C}=\text{N})$ ], 1594–1407 [ $\nu(\text{C}=\text{N}) + \nu(\text{C}_{\text{Ar}}=\text{C}_{\text{Ar}})$ ], 1065 [ $\nu(\text{N}=\text{N})$  azomethine].  $^1\text{H}$  NMR [DMSO;  $\delta$  (ppm)]: 7.14–8.68 (7H, H-rings), 12 (s, 1H, OH-iminole).  $^{13}\text{C}$  NMR [ $\text{dms}\text{-}d_6$ ;  $\delta$  (ppm)]: 161.91 [(C-iminole)]; 144.77 [C=N]; 122.03–150.79 [ $\text{C}_{\text{Ar}}$ ].

### 2.2. Synthesis of the complex of Fe(III) (1)

Introduce into a 100 mL flask containing 10 mL of methanol, 0.193 g (1 mmol) of the HL ligand. 5 mL of a methanol solution containing 0.1988 g (1 mmol) of the  $\text{FeCl}_2 \cdot 4\text{H}_2\text{O}$  was added to the resulting suspension. The mixture is stirred at room temperature for one hour. The clear solution obtained was filtered and the filtrate was left to slow evaporation. A few days later, brown crystals suitable for X-ray diffraction were recovered and washed with diethyl ether. IR ( $\nu$ ,  $\text{cm}^{-1}$ ): 3276; 3186; 3142; 3070; 1658; 1595; 1557; 1470; 1362; 1185; 1154; 1027; 829. UV-vis (Solution, DMF, nm): 219; 357; 421.  $\mu_{\text{eff}} (\mu_{\text{B}}) = 5.47$ .  $\Lambda$  (Solution, DMF,  $\Omega^{-1} \cdot \text{cm}^2 \cdot \text{mol}^{-1}$ ): fresh solution 50; two weeks later: 52.

### 2.3. X-ray data collection, structure determination, and refinement

Single crystals of **HL** and **1** were grown by slow evaporation of methanol solution of the corresponding complex. Suitable crystals were selected and mounted on a Rigaku Oxford Diffraction Super Nova diffractometer at the MoK $\alpha$  radiation. The crystal was kept at 299(2) K during data collection. Using *Olex2*[30], the structure was solved with the *SHELXT*[31] structure solution program using direct methods and refined with the *SHELXL*[32] refinement package. The crystallographic details of compounds **HL** and **1** are summarized in Table 1, and the bond lengths, bond angles of compounds are listed in Tables 3, respectively. Molecular graphics were generated using *ORTEP-3* [33].

**Table 1.** Crystal data and structure refinement for **HL** and **1**

Chemical formula	C <sub>11</sub> H <sub>9</sub> N <sub>3</sub> OS ( <b>HL</b> )	C <sub>12</sub> H <sub>13</sub> Cl <sub>3</sub> FeN <sub>3</sub> O <sub>2</sub> S ( <b>1</b> )
Mr	231.27	425.51
Crystal system	Monoclinic	Triclinic
Space group	<i>Cc</i>	<i>P-1</i>
Temperature (K)	299	299
a (Å)	10.0287 (4)	6.0713(1)
b (Å)	13.6033 (3)	10.1910(2)
c (Å)	8.5626 (3)	13.8844(2)
$\alpha$ (°)	90	84.995(1)
$\beta$ (°)	111.369 (4)	79.633(1)
$\gamma$ (°)	90	75.255(1)
V (Å <sup>3</sup> )	1087.83 (7)	816.44(2)
Z	4	2
Radiation type	Mo K $\alpha$	Mo K $\alpha$
$\mu$ (mm <sup>-1</sup> )	0.28	1.55
Crystal size (mm)	0.22 × 0.12 × 0.08	0.22 × 0.14 × 0.10
Tmin, Tmax	0.673, 1.000	0.673, 1.000
No. of measured	10035	15434
No. of independent reflections	1908	2897
No. of observed [ $I > 2\sigma(I)$ ] reflections	1721	2443
$R_{\text{int}}$	0.037	0.034
$R[F^2 > 2\sigma(F^2)]$	0.031	0.030
$wR(F^2)$	0.076	0.071
GOF	1.09	1.05
No. of reflections	1908	1897
No. of parameters	145	207

No. of restraints	2	3
$\Delta\rho_{\max}, \Delta\rho_{\min}$ (e $\text{\AA}^{-3}$ )	0.11, -0.18	0.45; -0.22

### 3. Results and discussion

#### 3.1. General study

The IR spectrum of the free ligand exhibits an intense band at  $1662\text{ cm}^{-1}$  attributed to the  $\nu_{\text{C=O}}$  vibration of the amide group [34]. The band observed at  $1630\text{ cm}^{-1}$  is assigned to the  $\nu_{\text{C=N}}$  vibrations of the imine group [35, 36] and the absorptions appearing in the  $1594\text{--}1407\text{ cm}^{-1}$  region are due to the  $\nu_{\text{C=C}}$  and  $\nu_{\text{C=N}}$  of the aromatic rings [37]. The absorption bands pointed in the region  $1393\text{--}1222\text{ cm}^{-1}$  are assigned to the  $\nu_{\text{C=N}}$  vibrations of the amide group and that observed at  $1065\text{ cm}^{-1}$  is due to the  $\nu_{\text{N-N}}$  of the azomethine moiety. The presence of the vibration of the C–N bond strictly indicates the existence of the ligand in its amide form in the solid state. This is confirmed by the presence of the  $\nu_{\text{N-H}}$  vibration at  $3428\text{ cm}^{-1}$ . The fairly broad band centered at  $3675\text{ cm}^{-1}$ , attributed to the  $\nu_{\text{O-H}}$  vibration of the molecules of free water suggests that the ligand is hydrated. The deformation vibrations of the C–H bonds of the aromatic rings are observed in the region  $999\text{--}740\text{ cm}^{-1}$ . The  $^1\text{H}$  and  $^{13}\text{C}$  NMR spectra of the ligand were recorded in  $\text{dms}\text{-}d_6$ . The  $^1\text{H}$  NMR spectrum reveals a signal at 12.00 ppm which is attributed to -OH protons. The fact suggests that an iminolisation of the ligand undergoes in solution [ $\text{NHC=O} \leftrightarrow \text{N=C(OH)-}$ ]. The signal observed at 8.78 ppm is assigned to the azomethine proton. The signals of the aromatic protons appear in the range 7.14–8.68 ppm. In the  $^{13}\text{C}$  NMR spectrum signal due to the azomethine carbon (H–C=N) atom is pointed at 144.57 ppm. The iminol carbon atom [ $\text{N=C(OH)-}$ ] [34] exhibits a signal at 161.91 ppm confirming the iminolisation. The electronic spectrum of the ligand recorded in a dilute solution of DMF shows an intense absorption at 323 nm attributed to the transitions  $\pi \rightarrow \pi^*$  of the aromatic nuclei and/or  $n \rightarrow \pi^*$  of the imine function of the ligand. Upon coordination, the IR spectrum of the complex shows a shift to low frequencies of the absorption band due to the  $\nu_{\text{C=N}}$  which is pointed at  $1610\text{ cm}^{-1}$ . The  $\nu_{\text{C=O}}$  value decrease from  $1662\text{ cm}^{-1}$  in the spectrum of the free ligand to  $1635\text{ cm}^{-1}$  in the spectrum of the complex. These observations are indicative of the involvement of the azomethine nitrogen atom and the oxygen atom of the amide group in the coordination to the metal. The band at  $3300\text{ cm}^{-1}$  is due to the  $\nu_{\text{O-H}}$  of the coordinated methanol. The molar conductivity measurements of the complex taken from a freshly prepared millimolar solution of DMF ( $50\ \Omega^{-1}\cdot\text{cm}^2\cdot\text{mol}^{-1}$ ) and two weeks later ( $52\ \Omega^{-1}\cdot\text{cm}^2\cdot\text{mol}^{-1}$ ) indicate that the complex is a neutral electrolyte according to Geary [38]. The slight increasing of the value is indicative of a good stability of the complex in DMF solution. The electronic spectrum of the complex recorded in DMF solution shows absorptions at 323 nm and 442 nm which are respectively attributed to the  $\pi \rightarrow \pi^*$  transitions of the aromatic ring and/or  $n \rightarrow \pi^*$  of the azomethine moiety and to charge transfers from the ligand to the metal. The complex show magnetic moment of  $5.47\ \mu_{\text{B}}$  corresponding to five unpaired electrons [39].

#### 3.1. Electrochemistry

The electrochemical properties of the ligand and of the complex were studied by the cyclic voltammetry method. The voltammograms were recorded from a solution of distilled water in which a

three-electrode system is used comprising a working electrode (GCE), an Ag/AgCl reference electrode and a stainless-steel wire counter electrode. The electrochemical study is particularly focused on the redox behavior of the ligand and the complex in the water solution used as electrolyte. A potential sweep in the potential range between -0.5 and 0.8 V with respect to Ag/AgCl, imposing a sweep rate equal to 20 mV/s was carried out for the ligand and the complex. The qualitative study of the voltammogram recorded in the solution of the ligand (**Figure 1**) revealed the presence of an anodic peak and a cathodic peak respectively at potentials 0.3 V and -0.2 V. These anodic and cathodic peaks are due respectively to the oxidation and reduction of the ligand.

The study of the electrochemical behavior of the complex shows the presence of a weak anodic peak at -0.14V followed by a large anodic peak around 0.42 V and a cathodic peak which exits at the -0.2 V potential. The band at potential around -0.2 V corresponds to the reduction of iron (III) to iron (II). This reduction probably results in the breaking of the metal-chloride bond according to the reaction  $[\text{Fe(III)(HL)(Cl)}_3(\text{MeOH})] + e^- \rightleftharpoons [\text{Fe(II)(HL)(Cl)}_2(\text{MeOH})] + \text{Cl}^-$ . We note that the potential difference is greater in the complex compared to that of the ligand. This shows the purely electronic aspect of the complex with respect to the ligand with the appearance of a redox couple at the highest potentials, thus showing the presence of a new couple in the solution which confirms the formation of the complex. The study of cyclic voltammograms with different scanning speeds between 10 and 45 mV/s (Figure 2) shows an increase in the intensities of the anodic and cathodic peak currents as a function of the scanning speed. Moreover, we note that the appearance of the curves is not distorted even at high sweep speeds (45 mV/s), which proves that there is no decomplexation. Then, the anodic potential peak shifts positively while the cathodic peak shifts towards negative potentials, showing that the electrochemical reaction is governed by an electron transfer process. Similarly, the spacing between peaks (Table 2) increases with scan speed, indicating an irreversible process. Both anodic and cathodic peak currents vary linearly with the square root of the sweep rate (Figure 3). These results suggest that the process is governed by an electrochemical diffusion process.

**Table 2. Summary of peak potentials at different scan rates**

V (mV/s)	V <sup>1/2</sup> (mV/s) <sup>1/2</sup>	E <sub>pox</sub> (V)	E <sub>pred</sub> (V)	ΔE <sub>p</sub> (V)
10	3.16	0.358	-0.100	0.458
15	3.87	0.370	-0.146	0.516
20	4.47	0.394	-0.170	0.564
25	5	0.410	-0.226	0.636
30	5.47	0.422	-0.240	0.662
35	5.91	0.432	-0.252	0.684
40	6.32	0.438	-0.266	0.704
45	6.70	0.448	-0.278	0.726

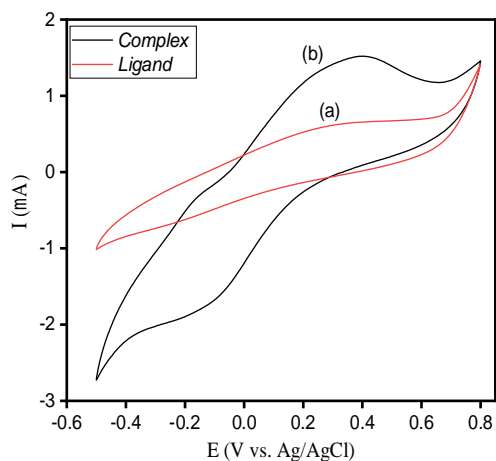


Figure 1. Cyclic voltammograms in distilled water on the glassy carbon electrode (GCE): (a) (Isonicotinic acid thiophene-2-ylmethylene-hydrazide) (b) [Fe(III)complex] with a scan rate of 20mV/s

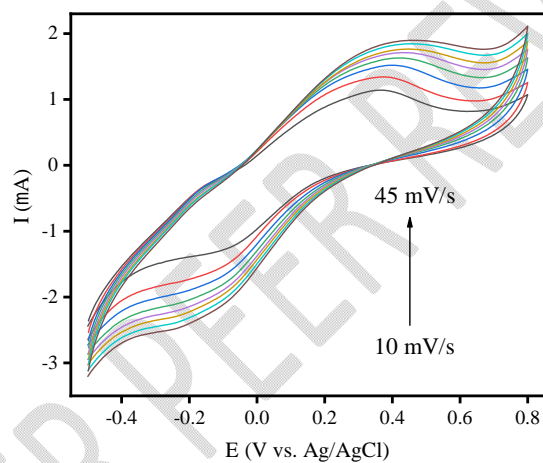


Figure 2. Cyclic voltammograms of the [Fe(III)] complex in distilled water on a vitreous carbon electrode (GCE) at different scanning speeds ( $v = 10$  to  $45$  mV/s)

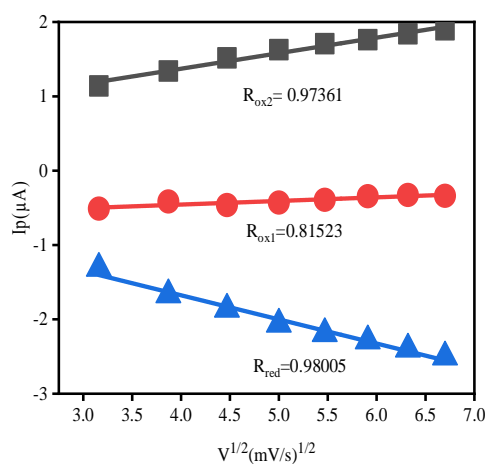


Figure 3. Calibration curve of peak currents versus square root of scan rate

**Table 3. Selected geometric parameters (Å, °)**

<b>HL</b>			
O1—C6	1.224 (4)	N3—C5	1.260 (4)
N3—N2	1.387 (3)	N2—C6	1.338 (4)
<b>1</b>			
Fe1—Cl3	2.4037 (7)	Fe1—O1	1.9776 (17)
Fe1—Cl1	2.3105 (7)	Fe1—O2	2.0948 (18)
Fe1—Cl2	2.3317 (7)	Fe1—N3	2.166 (2)
Cl1—Fe1—Cl3	168.85 (3)	O2—Fe1—Cl3	80.03 (5)
Cl1—Fe1—Cl2	94.36 (3)	O2—Fe1—Cl1	89.29 (6)
Cl2—Fe1—Cl3	91.39 (3)	O2—Fe1—Cl2	104.28 (6)
O1—Fe1—Cl3	92.51 (5)	O2—Fe1—N3	89.91 (8)
O1—Fe1—Cl1	97.03 (6)	N3—Fe1—Cl3	87.82 (6)
O1—Fe1—Cl2	90.01 (5)	N3—Fe1—Cl1	89.00 (6)
O1—Fe1—O2	163.92 (7)	N3—Fe1—Cl2	165.43 (6)
O1—Fe1—N3	75.50 (7)	Cl3—Fe1—Cl1	168.85 (3)

### 3.2. Structure of the ligand HL

The complex crystallizes in the monoclinic system with a space group *Cc*. The ORTEP diagram is depicted in Figure 4 and the selected bonds distances and angles are summarized in Table 3. The ligand adopts an *E* configuration with respect to C5=N3 bond. The carbonohydrazide moiety is almost coplanar with the thiophene ring, with dihedral angle of 4.09(1)° between their mean planes. The mean plane of the pyridine ring is severely twisted in opposite of the means planes of the thiophene ring and the carbonohydrazide moiety with dihedral angle values of 30.62(1)° and 29.13(1)°, respectively. The hydrazone moiety is quite planar with a maximum deviation from least-squares plane of 0.024(2) Å for the C6 atom. The C6=O1 bond length of 1.224 (4) Å, which is characteristic of double bond character, is indicative of the non-iminisation of the molecule. Only the keto form of the molecule is present. This observation is consolidated by the bond distances 1.338 (4) Å [N2—C6] and 1.387 (3) Å [N3—N2] which are indicative of single bond character and the bond distance of 1.260 (4) Å [N3—C5] which is double bond character. Those distances values are comparable to compound 3-(((thiophen-2-yl)methylidene)hydrazinyl)carbonylpyridinium chloride dihydrate [40]. The O1 and N3 are in *syn* conformation with respect to C6—N2 bond [O1—C6—N2—N3 = 5.6(5)°]. The sulfur atom of the thiophene ring and the N3 atom are in *syn* conformation with respect to the C4—C5 bond [S1—C4—C5—N3 = -1.6(5)]. The packing of the molecules reveals that the sheets of the different units are connected through intermolecular hydrogen bonding involving hydrazinyl -NH moiety and -CH as donor and pyridine nitrogen atom as acceptor (N2—H2...N1<sup>i</sup> and

C5—H5...N1<sup>i</sup> :  $i = x-1/2, -y+3/2, z-1/2$ ) resulting in  $ar_2^2(6)$  loop as shown in Figure 4. Additional intermolecular hydrogen bonding involving -CH as donor and azomethine nitrogen atom as acceptor (C1—H1...N3<sup>ii</sup>:  $ii = x-1/2, -y+1/2, z-1/2$ ) is observed. The molecular layers formed run almost parallel to the *ac* plane (Table 4 and Figure 5). These layers stack along the *b* axis.

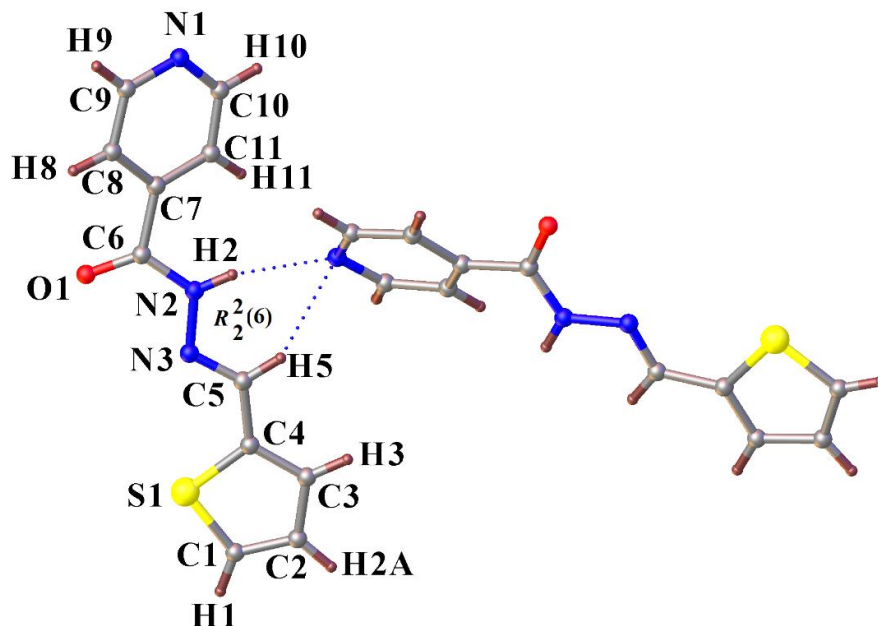


Figure 4. ORTEP plot (30% probability ellipsoids) showing the structure of HL

Table 4 : Hydrogen-bond geometry (Å, °) for HL

<i>D</i> —H... <i>A</i>	<i>D</i> —H	H... <i>A</i>	<i>D</i> ... <i>A</i>	<i>D</i> —H... <i>A</i>
N2—H2...N1 <sup>i</sup>	0.86	2.26	3.102 (4)	166.7
C5—H5...N1 <sup>i</sup>	0.93	2.67	3.497 (4)	149.2
C1—H1...N3 <sup>ii</sup>	0.93	2.69	3.612 (4)	171.2

Symmetry codes: (i)  $x-1/2, -y+3/2, z-1/2$ ; (ii)  $x-1/2, -y+1/2, z-1/2$ .

Table 5 : Hydrogen-bond geometry (Å, °) for 1

<i>D</i> —H... <i>A</i>	<i>D</i> —H	H... <i>A</i>	<i>D</i> ... <i>A</i>	<i>D</i> —H... <i>A</i>
O2—H2...Cl2 <sup>i</sup>	0.844 (9)	2.457 (11)	3.2445 (19)	155.7 (16)
C10—H10...Cl3 <sup>ii</sup>	0.93	2.81	3.350 (3)	118.0
C2—H2A...Cl1 <sup>iii</sup>	0.93	2.92	3.747 (3)	149.3
C12—H12B...Cl1 <sup>i</sup>	0.96	2.68	3.606 (3)	163.2
C12—H12C...Cl1	0.96	2.72	3.353 (4)	123.9
N1—H1...Cl3 <sup>ii</sup>	0.85 (4)	2.54 (3)	3.210 (3)	136 (3)

Symmetry codes: (i)  $x-1, y, z$ ; (ii)  $-x+2, -y+1, -z+1$ ; (iii)  $-x, -y+1, -z+2$ .

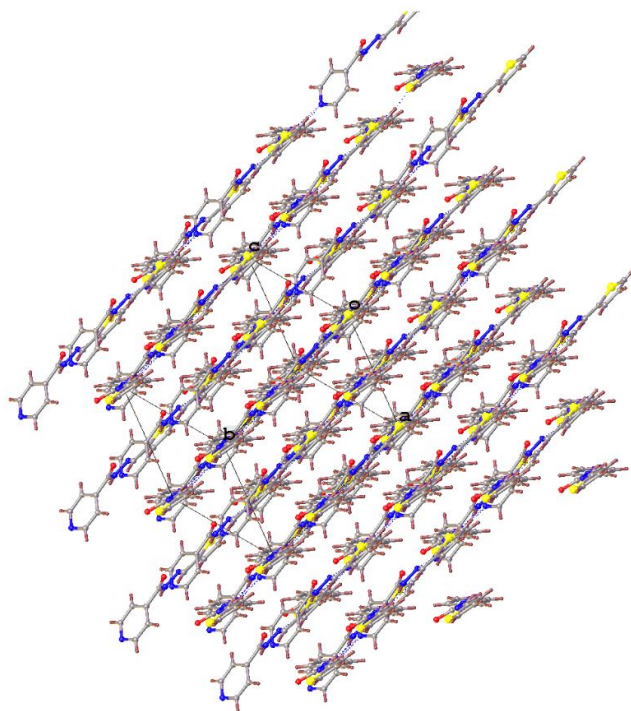


**Figure 5. Crystal packing observed for HL**

### 3.3. Structure of the Complex (1)

The complex crystallizes in the triclinic system with a space group P-1. The ORTEP diagram is depicted in Figure 6 and the selected bonds distances and angles are summarized in Table 3. The asymmetric unit contains one Fe(III) cation, one neutral ligand molecule, three coordinated chloride anions and one coordinated methanol molecule. The ligand acts in bidentate fashion through the carbonyl oxygen atom and the nitrogen azomethine atom. The sulfur atom of the thiophene ring and the nitrogen atom of the pyridine ring remain uncoordinated. The cation Fe(III) is in approximately octahedral coordination environments. The coordination sphere of Fe1 is filled by the carbonyl O1 [Fe1—O1 = 1.9776 (17) Å], the nitrogen atom N3 of the azomethine moiety [Fe1—N3 = 2.166 (2) Å]; the oxygen atom O2 of the coordinated methanol molecule [Fe1—O2 = 2.0948 (18) Å] and three coordinated chloride anions [Fe1—Cl1 = 2.3105 (7) Å; Fe1—Cl2 = 2.3317 (7) Å; Fe1—Cl3 = 2.4037 (7) Å]. The Fe—Cl bond lengths are slightly longer than the values reported for the complex FeLCl in which HL = 5-(2-(2-hydroxyphenyl)hydrazono)-2,2-dimethyl-4,6-dione [41]. The environment around Fe1 is best described as an octahedral geometry. The best equatorial plane of the polyhedron around the Fe(III) ion is constituted by two atoms from the two chelating Schiff base molecule, one oxygen atom from the coordinated methanol molecule and one terminal chloride anion (rms 0.00485) with the Fe(III) ion 0.0687(7) Å out of this plane. The axial positions are occupied by two terminal chloride anions Cl3—Fe1—Cl1 [168.85(3)°]. The angles around Fe1 deviate severely from the ideal values of 90 and 180° as expected for a perfect octahedron. The *cisoid* angles range from

87.32(6) to 94.36(3) °, while the *transoid* angles are 163.92(7)° [O1—Fe1—O2] and 165.43(6)° [N3—Fe1—Cl2].

Weak intermolecular hydrogen bond of type C—H...Cl [C12—H12C...Cl1] result in the formation of S(6) ring. Intermolecular hydrogen bonding of type O—H...Cl [O2—H2...Cl2<sup>i</sup>; i = x-1, y, z] and N—H...Cl [N1—H1...Cl3<sup>ii</sup>; ii = -x+2, -y+1, -z+1] link the molecules. Additional weak C—H...Cl [i.e. C2—H2A...Cl1<sup>iii</sup>; iii = -x, -y+1, -z+2] (Table 5) extended the structure into three-dimensional network (Figure 7).

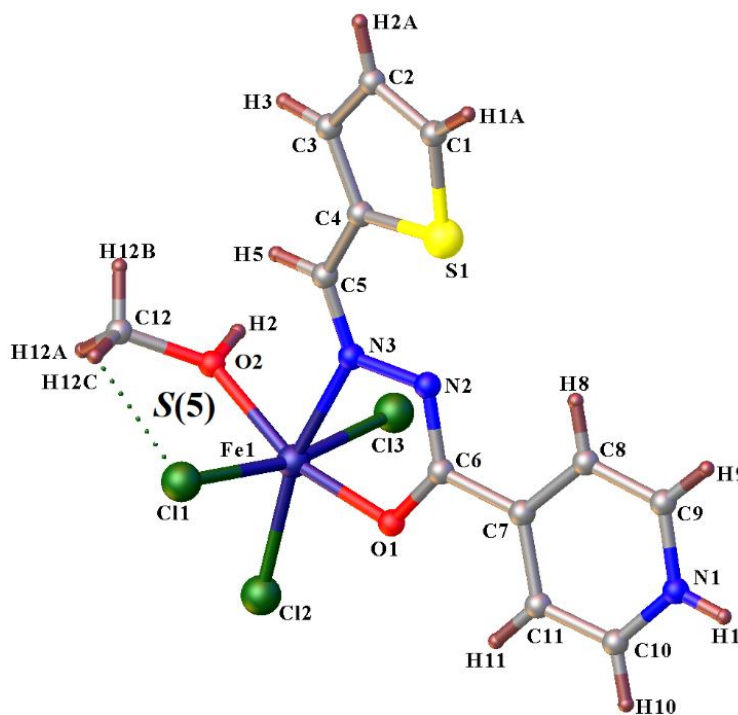
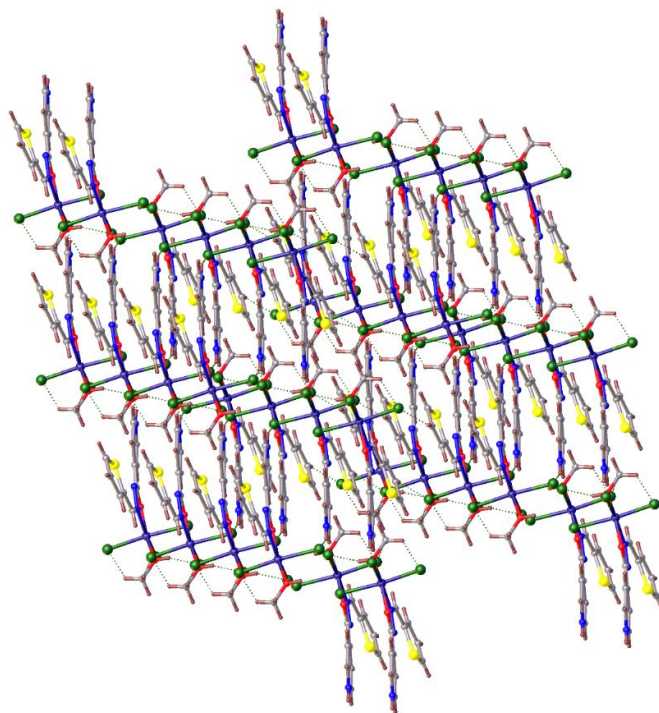


Figure 6. ORTEP plot (30% probability ellipsoids) showing the structure of 1



**Figure 7. Crystal packing observed in complex 1**

#### **4. Conclusion**

The HL ligand and its iron(III) complex were prepared and characterized by element analysis,  $^1\text{H}$  and  $^{13}\text{C}$  NMR, IR, UV-Vis spectroscopies, magnetic moment and molar conductivity. The structures of the ligand and the complex are established by single X-ray diffraction. The ligand, which possesses four potential coordination sites, acts only in bidentate fashion through the carbonyl oxygen atom and the azomethine nitrogen atom; the thiophene sulfur atom and the pyridine nitrogen atom remain uncoordinated. The ligand molecule reacts in its non-deprotonated mode. These complex of Fe(III) is neutral electrolyte in DMF solution. The magnetic moment value of the compound is indicative of a mononuclear complex as confirmed by the X-ray diffraction.

#### **Supplementary**

Additional material from the Cambridge Crystallographic Data Center comprises thermal parameters and remaining bond distances and angles (CCDC No. 2254003 (**HL**), 2254004 (**1**)). These data can be obtained free of charge from The Cambridge Crystallographic Data Center (CCDC), 12 Union Road, Cambridge CB2 1EZ, UK .

#### **References**

1. Ngororabanga JMV, Dembaremba TO, Mama N, Tshentu ZR. Azo-hydrazone tautomerism in a simple coumarin azo dye and its contribution to the naked-eye detection of  $\text{Cu}^{2+}$  and other potential applications. *Spectroch. Acta A Mol. Biomol. Spectrosc.* 2023; 289:122202. Available: <https://doi.org/10.1016/j.saa.2022.122202>
2. Zengin A, Serbest K, Emirik M, Özil M, Menteşe E, Faiz, Ö. Binuclear Cu(II), Ni(II) and Zn(II) complexes of hydrazone Schiff bases: Synthesis, spectroscopy, DFT calculations, and SOD mimetic activity. *J. Mol. Struct.* 2023;1278:134926. Available: <https://doi.org/10.1016/j.molstruc.2023.134926>
3. Tamboura, FB, Haba, PM, Gaye, M, Sall, AS, Barry, AH, Jouini, T. Structural studies of bis-(2,6-diacetylpyridine-bis-(phenylhydrazone)) and X-ray structure of its Y(III), Pr(III), Sm(III) and Er(III) complex. *Polyhedron.* 2004;23(7):1191–1197. Available: <https://doi.org/10.1016/j.poly.2004.01.014>
4. Raj BNB, Kurup MRP, Suresh E. Synthesis, spectral characterization and crystal structure of N-2-hydroxy-4-methoxybenzaldehyde-N'-4-nitrobenzoyl hydrazone and its square planar Cu(II) complex. *Spectroch. Acta A Mol. Biomol. Spectrosc.* 2008;71(4):1253–1260. Available: <https://doi.org/10.1016/j.saa.2008.03.025>
5. Lumme P, Elo H, Jänne J. Antitumor activity and metal complexes of the first transition series. Trans-bis(salicylaldoximato)copper(II) and related copper(II) complexes, a novel group of potential antitumor agents. *Inorg. Chim. Acta.* 1984;92(4):241–251. Available: [https://doi.org/10.1016/S0020-1693\(00\)80045-6](https://doi.org/10.1016/S0020-1693(00)80045-6)
6. Shahverdizadeh GH, Tiekink ERT, Mirtamizdoust B. *catena*-Poly[[lead(II)- $\mu$ -N-[1-(pyridin-2-yl- $\kappa$ N)ethylidene]isonicotinohydrazidato- $\kappa^3$ N,O:N'] perchlorate]. *Acta Crystallogr, Sect. E: Crystallogr, Commun.* 2011;67(12):m1727–m1728. Available: <https://doi.org/10.1107/S1600536811046691>
7. Shahverdizadeh GH, Tiekink ERT, Mirtamizdoust B. *catena*-Poly[[[bis(methanol- $\kappa$ O)lead(II)- $\mu$ -N-[1-(pyridin-2-yl- $\kappa$ N)ethylidene]isonicotinohydrazidato- $\kappa^3$ N,O:N'] perchlorate]. *Acta Crystallogr, Sect. E: Crystallogr Commun.* 2011;67(12):m1729–m1730. Available: <https://doi.org/10.1107/S1600536811046769>
8. Sall O, Tamboura FB, Sy A, Barry AH, Thiam EI, Gaye M, Ellena J. Crystal structures of two  $\text{Cu}^{\text{II}}$  compounds: *catena*-poly[[chloridocopper(II)]- $\mu$ -N-[ethoxy(pyridin-2-yl)methylidene]-N-[oxido(pyridin-3-yl)methylidene]hydrazine- $\kappa^4$ N,N',O:N"] and di- $\mu$ -chlorido-1:4 $\kappa^2$ Cl:Cl-2:3 $\kappa^2$ Cl:Cl-dichlorido-2 $\kappa$ Cl,4 $\kappa$ Cl-bis[ $\mu_3$ -ethoxy(pyridin-2-yl)methanolato-1:2:3 $\kappa^3$ O:N,O;1:3:4 $\kappa^3$ O:N,O]bis[ $\mu_2$ -ethoxy(pyridin-2-yl)methanolato-1:2 $\kappa^3$ N,O;3:4 $\kappa^3$ N,O;O]tetracopper(II). *Acta Crystallogr, Sect. E: Crystallogr, Commun.* 2019;75(7):1069–1075. Available: <https://doi.org/10.1107/S2056989019008922>
9. Faye M, Sow MM, Gaye PA, Dieng M, Gaye M. Crystal structures of bis-{N-[1-(pyridin-2-yl- $\kappa$ N)ethylidene]nicotine hydrazide- $\kappa^2$ N,O}cobalt(II)bis(perchlorate) dihydrate and bis-{N'-[1-(pyridin-2-yl- $\kappa$ N)ethylidene]nicotinohydrazide- $\kappa^2$ N,O}copper(II) perchlorate. *Eur. J. Chem.* 2021;12(2):159–164. Available: <https://doi.org/10.5155/eurjchem.12.2.159-164.2074>

10. Danilescu O, Bourosh PN, Petuhov O, Kulikova OV, Bulhac I, Chumakov YM, Croitor L. Crystal Engineering of Schiff Base Zn(II) and Cd(II) Homo- and Zn(II)M(II) (M = Mn or Cd) Heterometallic Coordination Polymers and Their Ability to Accommodate Solvent Guest Molecules. *Molecules*. 2021;26(8):2317.  
Available:<https://doi.org/10.3390/molecules26082317>
11. Liu H-J, Yi R, Chen D-M, Huang C, Zhu B-X. Self-Assembly by Tridentate or Bidentate Ligand: Synthesis and Vapor Adsorption Properties of Cu(II), Zn(II), Hg(II) and Cd(II) Complexes Derived from a Bis(pyridylhydrazone) Compound. *Molecules*. 2021;26(1):109.  
Available:<https://doi.org/10.3390/molecules26010109>
12. Jiang T, Tian L-C, Mo X-J, Chen D-M, Huang C, Zhu B-X, Zhu C. Synthesis, structural diversity, DFT and luminescence properties of Ni(II), Zn(II) and Cd(II) complexes derived from a 2, 2'-bipyridyl hydrazone Schiff base. *Polyhedron*. 2022;221:115861.  
Available:<https://doi.org/10.1016/j.poly.2022.115861>
13. Zhang K, Yang Z, Wang B, Sun S-B, Li Y-D, Li T, Liu Z, An, J. A highly selective chemosensor for Al<sup>3+</sup> based on 2-oxo-quinoline-3-carbaldehyde Schiff-base. *Spectroch. Acta A Mol. Biomol. Spectrosc.* 2014;124:59–63.  
Available:<https://doi.org/10.1016/j.saa.2013.12.076>
14. Fan L, Li T, Wang B, Yang Z, Liu C. A colorimetric and turn-on fluorescent chemosensor for Al(III) based on a chromone Schiff-base. *Spectroch. Acta A Mol. Biomol. Spectrosc.* 2014;118:760–764.  
Available:<https://doi.org/10.1016/j.saa.2013.09.062>
15. Li H, Xu G-C, Zhang L, Guo J-X, Jia D-Z. Structural diversity and properties of four complexes with 4-acyl pyrazolone derivative. *Polyhedron*. 2013;55:209–215.  
Available:<https://doi.org/10.1016/j.poly.2013.03.024>
16. Yang Z-Y. Synthesis, Characterization and Scavenger Effects on O<sub>2</sub> – of 3d Transition Metal Complexes of Isonicotinoyl Hydrazone Derived from Isoniazid with PMBP. *Synth. React. Inorg. Met.-Org. Chem.* 2000;30(7):1265–1271.  
Available:<https://doi.org/10.1080/00945710009351832>
17. Devi J, Kumar S, Kumar D, Jindal DK, Poornachandra Y. Synthesis, characterization, in vitro antimicrobial and cytotoxic evaluation of Co(II), Ni(II), Cu(II) and Zn(II) complexes derived from bidentate hydrazones. *Res. Chem. Intermed.* 2022;48(1):423–455.  
Available:<https://doi.org/10.1007/s11164-021-04602-8>
18. Hayat M, Khan KM, Saeed S, Salar U, Khan M, Baig T, Ahmad A, Parveen S, Taha, M. Antimicrobial Activities of Synthetic Arylidine Nicotinic and Isonicotinic Hydrazones. *Lett. Drug Des. Discovery*. 2018;15(10):1057–1067.  
Available:<https://doi.org/10.2174/1570180814666170914120337>
19. Kargar H, Kaka-Naeini A, Fallah-Mehrjardi M, Behjatmanesh-Ardakani R, Amiri RH, Munawar KS. Oxovanadium and dioxomolybdenum complexes: synthesis, crystal structure, spectroscopic characterization, and applications as homogeneous catalysts in sulfoxidation. *J. Coord. Chem.* 2021;74(9–10):1563–1583.  
Available:<https://doi.org/10.1080/00958972.2021.1915488>

20. Kargar H, Kargar K, Fallah-Mehrdadi M, Munawar KS. Syntheses, characterization, and catalytic potential of novel vanadium and molybdenum Schiff base complexes for the preparation of benzimidazoles, benzoxazoles, and benzothiazoles under thermal and ultrasonic conditions. *Monatsh. Chem.* 2021;152(6):593–605.  
Available: <https://doi.org/10.1007/s00706-021-02780-0>
21. Iliev I, Kontrec D, Detcheva R, Georgieva M, Balacheva A, Galić N, Pajpanova T. Cancer cell growth inhibition by aroylhydrazone derivatives. *Biotechnol. Equip.* 2019;33(1):756–763.  
Available: <https://doi.org/10.1080/13102818.2019.1608302>
22. Ashiq U, Jamal RA, Mesaik MA, Mahroof-Tahir M, Shahid S, Khan KM. Synthesis, Immunomodulation and Cytotoxic Effects of Vanadium (IV) Complexes. *Med. Chem.* 2014;10(3):287–299.  
Available: <https://doi.org/10.2174/15734064113099990033>
23. Diouf O, Gaye M, Sall AS, Tamboura F, Barry AH, Jouini T. Crystal structure of diaqua-2,6-diacetylpyridine-bis(acetylhydrazone)copper(II) complex dinitrate hydrate,  $[\text{Cu}(\text{C}_{13}\text{H}_{17}\text{N}_5\text{O}_2)(\text{H}_2\text{O})_2](\text{NO}_3)_2 \cdot \text{H}_2\text{O}$ , Z. Krist.-New Cryst. St. 2001;216(1–4):443–444.  
Available: <https://doi.org/10.1524/ncrs.2001.216.14.443>
24. Haba PM, Gaye M, Sall AS, Barry AH, Jouini T. Crystal structure of aquabis(4-methyl-5-formyl-imidazolofuranoylhydrazone)-(trinitrato)praseodymium(III) monohydrate,  $\text{Pr}(\text{H}_2\text{O})(\text{C}_9\text{H}_{10}\text{O}_2\text{N}_4)_2(\text{NO}_3)_3 \cdot \text{H}_2\text{O}$ . Z. Krist.-New Cryst. St. 2004;219(2):106–108.  
Available: <https://doi.org/10.1524/ncrs.2004.219.2.106>
25. Sy A, Dieng M, Thiam IE, Gaye M, Retailleau P. Dichlorido{*N*-[phenyl(pyridin-2-yl- $\kappa$ N)methylidene]isonicotinohydrazide- $\kappa^2$ N,O}zinc. *Acta Crystallogr, Sect. E: Crystallogr, Commun.* 2013;69(2):m108.  
Available: <https://doi.org/10.1107/S1600536813001281>
26. Sow MM, Diouf O, Gaye M, Sall AS, Castro G, Pérez-Lourido P, Valencia L, Caneschi A, Sorace L. Sheets of Tetranuclear Ni(II) [2 × 2] Square Grids Structure with Infinite Orthogonal Two-Dimensional Water–Chlorine Chains. *Cryst. Growth Des.* 2013;13(10):4172–4176.  
Available: <https://doi.org/10.1021/cg400885f>
27. Tamboura FB, Diouf O, Barry AH, Gaye M, Sall, AS. Dinuclear lanthanide(III) complexes with large-bite Schiff bases derived from 2,6-diformyl-4-chlorophenol and hydrazides: Synthesis, structural characterization and spectroscopic studies. *Polyhedron.* 2012;43(1):97–103.  
Available: <https://doi.org/10.1016/j.poly.2012.06.025>
28. Seck TM, Gaye PA, Diouf O, Thiam IE, Gaye, M. Synthesis, Spectroscopic Studies, and Crystal Structure Determination of a Novel Mn(II) Complex with *N,N*-1,5-bis(2-acetylpyridinyl)carbonohydrazone Ligand. *Chem. Afr.* 2020;3(4):949–954.  
Available: <https://doi.org/10.1007/s42250-020-00140-9>
29. Faye M, Gaye PA, Sow MM, Dieng M, Tamboura FB, Gruber N, Gaye, M. Synthesis, Characterization and Single Crystal X-ray Crystallography of Nd(III) and Pr(III) Complexes with

- the Tridentate Schiff Base Ligand *N*-(1-(pyridin-2-yl)ethylidene)nicotinothiohydrazide. *Earthline J. Chem. Sci.*2021;6(1):99–117.  
Available:<https://doi.org/10.34198/ejcs.6121.99117>
30. Dolomanov OV, Bourhis LJ, Gildea RJ, Howard JAK, Puschmann H. OLEX2: a complete structure solution, refinement, and analysis program. *J. Appl. Crystallogr.*2009;42(2):339–341.  
Available:<https://doi.org/10.1107/S0021889808042726>
  31. Sheldrick GM. Integrated space-group and crystal-structure determination. *Acta Crystallogr, Sect. A: Found. Adv.*2015;71:3–8.  
Available:<https://doi.org/10.1107/S2053273314026370>
  32. Sheldrick GM. Crystal structure refinement with SHELXL. *Acta Crystallogr, Sect. C: Struct. Chem.*2015;71:3–8.  
Available:<https://doi.org/10.1107/S2053229614024218>
  33. Farrugia LJ. ORTEP-3 for Windows - a version of ORTEP-III with a Graphical User Interface (GUI). *J. Appl. Crystallogr.*1997;30:565.  
Available:<https://doi.org/10.1107/S0021889897003117>
  34. Stani C, Vaccari L, Mitri E, Birarda G. FTIR investigation of the secondary structure of type I collagen: new insight into the amide III band. *Spectroch. Acta A Mol. Biomol. Spectrosc.* 2020;229:118006.  
Available:<https://doi.org/https://doi.org/10.1016/j.saa.2019.118006>
  35. Casellato U, Guerriero P, Tamburini S, Vigato PA, Benelli C. Mononuclear, homo- and heteropolynuclear complexes with acyclic compartmental Schiff bases. *Inorg. Chim. Acta.* 1993;207(1):39–58.  
Available:[https://doi.org/10.1016/S0020-1693\(00\)91454-3](https://doi.org/10.1016/S0020-1693(00)91454-3)
  36. Aruna VAJ, Alexander V. Synthesis of lanthanide(III) complexes of a 20-membered hexaaza macrocycle. *J. Chem. Soc., Dalton Trans.* 1996:1867–1873.  
Available:<https://doi.org/10.1039/DT9960001867>
  37. Ran J-W, Zhang S-Y, Hu B, Xu B, Li Y. Trinuclear and mononuclear nickel(II) complexes incorporating tridentate 2-[(pyridine-2-ylimine)methyl]phenol ligand: Syntheses, crystal structures and magnetic properties. *Inorg. Chem. Commun.*2008;11(12):1474–1477.  
Available:<https://doi.org/10.1016/j.inoche.2008.10.013>
  38. Geary WJ. The use of conductivity measurements in organic solvents for the characterisation of coordination compounds. *Coord. Chem. Rev.*1971;7(1):81–122.  
Available:[https://doi.org/10.1016/S0010-8545\(00\)80009-0](https://doi.org/10.1016/S0010-8545(00)80009-0)
  39. Chandra S, Gupta LK. Spectroscopic approach in characterization of chromium(III), manganese(II), iron(III) and copper(II) complexes with a nitrogen donor tetradentate, 14-membered azamacrocyclic ligand. *Spectroch. Acta A Mol. Biomol. Spectrosc.*2005;61(9):2139–2144.  
Available:<https://doi.org/10.1016/j.saa.2004.06.060>
  40. Chandrasekaran T, Suresh M, Novina JJ, Padusha MKSA, Vasuki G, Kasthuri B. Crystal structure of 3-(((thiophen-2-yl)methylidene)hydrazinyl)carbonylpyridinium chloride dihydrate.

Acta Crystallogr, Sect. E: Crystallogr Commun.2014;70(9):o976–o977.  
Available:<https://doi.org/10.1107/S1600536814017565>

41. Kumar SS, Sreepriya RS, Biju S, Sadasivan V. Synthesis, crystal structure and spectroscopic studies of trivalent Fe(III) and mixed valent ion-pair Co(II,III) complexes with 5-(2-(2-hydroxyphenyl)hydrazono)-2,2-dimethyl-4,6-dione. J. Mol. Struct.2019;1197:235–243.  
Available:<https://doi.org/10.1016/j.molstruc.2019.07.049>

UNDER PEER REVIEW